Proceedings of the ASME 2013 International Mechanical Engineering Congress and Exposition
IMECE2013
November 15-21, 2013, San Diego, California, USA

IMECE2013-65688

PRECISION AND ENERGY USAGE FOR ADDITIVE MANUFACTURING

Lee Clemon
Department of Mechanical Engineering
University of California
Berkeley, California 94720

Anton Sudradjat
Department of Mechanical Engineering
University of California
Berkeley, California 94720

Maribel Jaquez
Department of Mechanical Engineering
University of California
Berkeley, California 94720

Aditya Krishna
Department of Mechanical Engineering
University of California
Berkeley, California 94720

Marwan Rammah
Department of Mechanical Engineering
University of California
Berkeley, California 94720

David Dornfeld
Department of Mechanical Engineering
University of California
Berkeley, California 94720

ABSTRACT

Market pressures on manufacturing enterprises incentivize minimum resource consumption while maintaining part quality. Facilities with advanced manufacturing tools often utilize rapid prototyping for production of complicated or specialty parts. Additive manufacturing offers an alternative to traditional production methods which are often time and resource expensive. This study aims to explore part quality and energy usage for additive manufacturing through a focused study of Fused Deposition Modeling and Photopolymer Jetting technologies. A control part is developed for maintaining test consistency across different machines. The control part design consists of various positive and negative features including width varied slots and walls, ramps, and curved features so that the manufacturing of different surfaces may be investigated. Several different machine models are tested to evaluate precision for a variety of applications. Part quality is quantified by measuring the surface roughness in two directions for the control test part printed on each machine. Qualitatively, part quality is assessed by positive and negative feature resolution. High quality machines resolve features closely to design specifications. Lower quality machines do not resolve some features. In addition to exploring the effects of advertised print precision, layup density is varied on two machines. Advertised print resolution does not well represent the achievable feature sizes found in this study. Energy usage is quantified by measuring electricity demands while printing the control part on each of the five different machines. Power consumption in additive manufacturing is found to follow a distinct pattern comprised of standby, warm up, printing and idle phases. Measurement and analysis suggest a relationship between the precision of these machines and their respective energy demand. Part quality is found to generally improve with increased initial and process resource investment. The energy and quality assessment methods developed in this study are applicable to a greater variety of additive manufacturing technologies and will assist designers as additive manufacturing becomes more production friendly. The presented data also provides designers and production planners insight for improvements in the process decision making.

INTRODUCTION

Additive Manufacturing (AM) is the process of joining material to create 3D objects, typically layer by layer. As a result of the additive approach, AM can build complex geometries that other methods are not capable of fabricating [1].

One challenge AM faces is the lack of developed standards. Intact standards drive increased quality and market acceptance, thus promoting the adaptation of technologies. An ASTM International Committee F42 on AM Technologies was formed in 2009 to establish industry standards for the adoption and further implementation of AM [2]. Process characterization of printing energy to material weight is available in the literature but there is a lack of characterizing printing energy in regards to feature quality [3], [4]. This paper aims to explore quality and energy usage for AM and fill this white space in the knowledge base. The motivation for the research stems from the work done in [5], [6], [7], [8], and [9] which conclude that machine tools operate at fixed energy levels during different phases of operation. However, most related research until now has focused on subtractive manufacturing and therefore, there is a need to explore the applicability of this principle to AM.

Developing an energy standard for AM similar to the baseline energy consumption (BEC) metric currently established for lathe technologies will also aid understanding of the energy impact of AM [10]. One major benefit for standardizing the energy impact of AM is the ability to compare AM processes on a basis of energy efficiency for a given part quality.

In this study, part quality is assessed by measuring feature completion and surface roughness. Energy is assessed by measuring the electrical energy consumption of different AM machines when producing a control part. Fused Deposition Modeling (FDM) and Photopolymer Jetting are the two AM processes presented herein.

METHODOLOGY

The implemented testing methods allow for general application. The developed control part and print volume definition are suitable for broad application. Part quality assessment techniques adopted here sufficiently describe machine achievements. Energy measurement and data analysis are also scientifically sound.

Testing a total of five different machines provide the ability to explore a range of different levels of precision. The FDM testing is done on 4 different machine models: Dimension BST1200, Dimension SST1200es, uPrint by Dimension, and a MakerBot Replicator 2. The first three machines are supported by Stratasys, Inc, whereas the final machine is supported by MakerBot Industries. The FDM process extrudes liquefied thermoplastic material from a temperature controlled heated nozzle that deposits material in thin beads that bond together to form layers [3]. Photopolymer Jetting testing is done on an Objet Connex350 machine. In Photopolymer Jetting, a polymer resin is deposited to form a layer, a leveling roller passes over to smooth the surface, and afterwards a UV light passes over the layer and cures the polymer into a solid [11].

To account for differences in machine design, the printing volume is assigned X, Y and Z axes. The X-Y plane is defined as the rectangular surface on which the parts are printed. The Z-axis is defined orthogonal to the printing surface. Some machines move the X-Y surface in the Z direction while the printer head moves in the X and Y directions. Other machines fix the X-Y surface and move only the printer head. Generally, the normal of the X-Y plane is parallel to gravity.

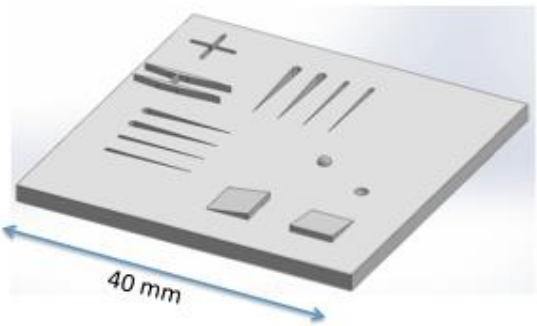

Fig. 1: CAD Model of Control Part

In order to accurately compare the part quality and electrical energy consumption of different AM machines, a control part was designed using SolidWorks. Other researchers have produced a part for general AM testing which was not available at the time of these experiments [12]. The part design consists of various features to test the accuracy of each printer. Slot and ramp features are duplicated in two orthogonal directions to reveal quality preferences for the X and Y axes. Slots and walls with varying thickness are incorporated to identify the minimum feature size each machine can resolve. Ramps and spherical shapes were chosen to determine the variations of printed 3D surfaces to designed flat surfaces. The feature sizes range from the millimeter scale to the micrometer scale to determine minimum resolution. The CAD model of the design can be seen in fig. 1. Slots are each 10 mm in length. Each direction contains two "wide" slots varying in width from 0.5 mm to 0 mm and two "narrow" slots varying from 0.25 mm to 0 mm. Slot width from a finite value to zero allows for determination of the minimum achievable slot width, hence the minimum wall separation achievable. Ramp features are 2.5 mm tall with a slope of 0.5 mm/mm. Two positive features, i.e. walls, vary in width from 0 mm to 0.25 mm. A third wall, orthogonal to the first two, is a constant 0.1 mm wide. A flat space is intentionally left to measure surface roughness and assess flatness. The part designed in this experiment is well suited to the adopted quality measurements. This control part was printed using a variety of 3D printers.

Ideally, all of the parts would be printed using the same material. However, different printers may only use particular printing materials. These materials are generally proprietary variations on known plastics (i.e. ABS plastic). The materials in this experiment all have similar mechanical properties. The MakerBot Replicator 2 and Dimension BST1200 use ABS plastic. The other FDM machines all use Stratasys' ABS+ model material with either Stratasys soluble support or breakaway support materials. The Objet Connex350 uses VeroClear as the model material. All of these materials are advertised as being ABS or "ABS-like" therefore it is assumed that the properties of the materials are similar and any differences are neglected in this analysis. When printing with the Dimension BST1200 and uPrint models, it is possible to adjust the density of the final part. Printing full density or "solid" material and printing low density or "sparse" material is tested to investigate differences in energy demand between the two settings in these machine models.

Energy Measurement and Processing

Electricity is delivered through a single phase 120V wall outlet. Voltage and current measurements are sampled at 10 Hz using a Yokogawa CW240 connected inline between the machine in question and the wall. Each machine is turned off for a minimum of 8 hours prior to initial energy measurements. This allows for adequate cool down time and accurate measurement of the energy required to start up the

machine. The machine is run for at least 60 seconds before and after each part is printed to capture fluctuations and phases outside of printing. Additional measurement of non-print time power demand cycles is conducted to verify differences from print time loads. In addition to measuring the energy consumption for printing the custom part in the FDM machines, the effect of part orientation on energy consumption for the Objet Connex350 machine is also explored.

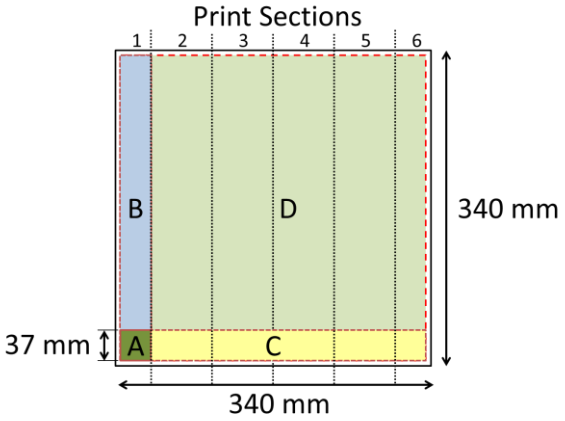

Fig. 2: Overlay of energy demand test part areas for Objet Connex350. Parts B (37x340 mm) and C (340x37 mm) are the same area, Parts A (37 mm) and D (340 mm) are square.

The Objet Connex350 machine's printable 340 x 340 mm area is divided into six quadrants that each print individually. Due to this design, part orientation could affect print time and energy consumption. In order to analyze this design, a set of five test parts of equal height in the Z-direction are printed with varying X and Y dimensions, as well as orientation. The energy used to print a square part with dimensions 37 x 37 mm, labeled part A in fig. 2, fits in the first section is compared to the energy used to print the full length of the first section, 37 x 340 mm, labeled part B in fig. 2. Similarly, part C in fig. 2 is the same size as part B, but crosses through all of the sections. Part D in fig. 2 provides a data point for comparison of part pairs BD and AC to highlight section transition energy demands. Finally, the control part used for all machines and the intermediate 40 x 100 mm part provide additional data points to check estimates derived from parts A, B, C, and D.

Instantaneous power data collects while each test part prints. During the tests, the machine displays phase transitions, which are noted for comparison with power demand changes. The test noted phase transitions and raw power data are plotted together for visual inspection and verification. Minor differences found in the testing notes and actual power state changes are corrected to discover true operation phases. The testing notes and significant power state changes are analyzed revealing a common pattern across all of the machines, further described in the results.

Quality Measurement and Assessment

The quality of the printed parts is quantitatively captured in surface roughness measurements. An ASIQ Tencor AS500 profilometer set to 100X magnification is used to measure the surface roughness of each part. Measuring Ra in both the X and Y directions captures axial quality preferences. In addition to surface roughness, the features of the control part are captured using a digital microscope. A digital microscope records section images of the part with a reference ruler. The features are measured using the number of pixels in feature spans calibrated to the reference ruler. The different feature measurements are compared to the part design on SolidWorks for an assessment of completeness. For example, the length of the slots and smallest gaps between their walls are measured in order to determine the minimum size slot each machine is able to print. Similarly, the dome feature is measured and compared to the design diameter. In addition to quantifying the resolution of some features, a qualitative assessment of the functionality is also discussed.

The results are combined to investigate the potential relationship between the quality of parts produced and the energy requirements of the different machines with the hypothesis that more precise parts require greater energy inputs.

RESULTS

Energy Results and Description

A common pattern across machines of differing manufacturers and technologies was identified. To describe this pattern, a model was adapted from the Baseline Energy Consumption standard for turning in [10]. This model describes phases or energy levels for a machine. In this work all of the machines proceed through the following phases: standby, warm up, printing, and idle.

1. Standby: The machine is on; powering only the minimum number of components. Parts cannot print in this state.

2. Warm up: The machine is heating the necessary components to the requisite temperature for the printing operation. This phase also includes sub-phases that vary by machine and with time, such as calibration.

3. Printing Phase: The machine prints the part during this phase. The phase in interspaced with high frequency and low frequency variations. Low frequency variations are attributed to the intermittent switching of the heater between on and off states. This is necessary to keep the material in the requisite molten state. The high frequency variations are attributed to movement of the axes, which are stationary in other phases.

4. Idle Phase: The machine is in the ready-to-print state but is not printing. The heating elements continue to cycle, keeping the material in a state ready to be printed. Thus, low frequency variations were observed during this phase

This framework defines the four states such that a machine cannot transition directly between Standby and Printing, but all other state transitions may occur. The warm

up phase may be encountered when the machine is first switched on or as an intermediate between standby and printing. At a machine's initial startup, the warm up phase may be longer than at other times depending how long it was powered off. The requisite temperature for the material is maintained via heating cycles in subsequent phases such as printing and idling. Each phase was considered independently for the analysis. For phases without major fluctuations, the duration of the phase as well as the mean are calculated. For phases with large fluctuations, the underlying waveform is identified to be square. For these square waves, the mean energy levels are calculated at the 'high' power band and the 'low' power band along with the fraction of time spent at each level. The weighted mean for power consumption is then calculated. Mean power demand is calculated for components and subassemblies that are easily identified in the data.

Effect of transition periods

Transition periods are defined as the duration of time the machine took to change from one phase to another. As expected, the variations during this phase are not uniform with unexpected variations. Data analysis including these transition periods into corresponding phases did not appreciably affect the results. This enhances the completeness of information used in the model.

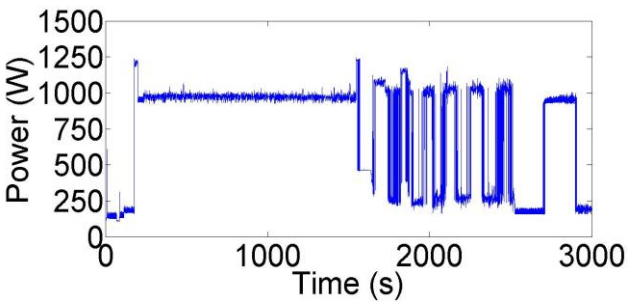

Fig. 3: Power profile for the Dimension BST 1200 with part density set to solid showing standby, warm up, printing and idle phases

Raw power consumption for the Dimension BST1200 with the part density set to solid and the Objet Connex350 can be seen in fig. 3 and fig. 4, respectively. Similar graphs are collected for all of the machines and varied part density settings. This data,, when split into the identified phases, yields the results in Tab. 1. Subtracting the contributions from idle and standby phases from the total power during the printing phase gives the power consumption attributed to the printing process itself. It is important to note that for the solid part on the Dimension BST1200 the duty cycle for heating increases in frequency. In the Objet Connex350, the distinction between motion, lighting, and heating power is obfuscated. A higher duty cycle for heating in the Objet Connex350 is inferred to account for technological and precision differences. The energy consumed during each phase is calculated by obtaining the area under the power curve for that phase.

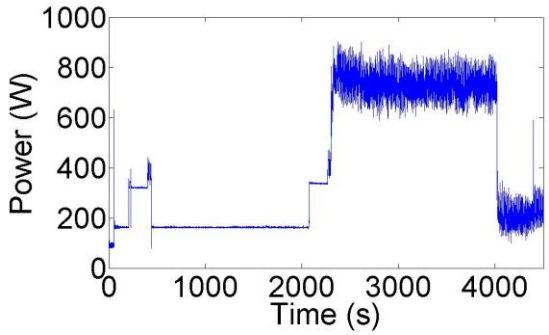

Fig. 4: Objet Connex350 instantaneous power profile showing standby, warm up, printing and idle phases

In the equations deriving energy usage for various phases, the following notation is used.

Variable definitions:

t = time

$\overline{P}$ = average measured power at a given state during a given phase

Q = printing process power, excluding standby, warm up and heating elements

N = number of parts produced without entering standby

Subscript definitions:

H = high band of samples
L = low band of samples
P = printing phase
I = idle phase
S = standby phase
o = total time of phase
avg = average value for the phase
$part$ = refers to an individual part

An example of how the defined variables and subscripts combine is the time spent in the high power band during the printing phase, $t_{H,P}$, divided by the total time of the printing phase, $t_{o,P}$, is denoted:

$$\frac{t_{H,P}}{t_{o,P}} \equiv \quad \text{fraction of printing phase at high band}$$

The standby and warm up power demands were measured directly and are presented in tab. 1. The power demand for the idle phase is calculated by subtracting the standby power demand from the measured idle power demand. The power demand for the standby phase and the idle phase are shown in eqn. (1) and eqn. (2), respectively.

$$Q_{avg,S} = Q_{H,S} + Q_{L,S} = \overline{P}_{H,S} * \frac{t_{H,S}}{t_{o,S}} + \overline{P}_{L,S} * \frac{t_{L,S}}{t_{o,S}} \quad (1)$$

$$Q_{avg,I} = \overline{P}_{H,I} * \frac{t_{H,I}}{t_{o,I}} + \overline{P}_{L,I} * \frac{t_{H,I}}{t_{o,I}} - Q_{avg,S} \quad (2)$$

Finally, the power demand for the printing phase is then calculated by subtracting the idle and standby power demands from the measured power demand during printing. Separating this into the high and low bands for each phase yields Eqn. (3) , then the sum of the two bands gives the overall average power demand for printing alone, Eqn. (5).

$$Q_{H,P} = \overline{P}_{H,P} * \frac{t_{H,P}}{t_{o,P}} - Q_{H,I} - Q_{H,S} \quad (3)$$

$$Q_{L,P} = \overline{P}_{L,P} * \frac{t_{L,P}}{t_{o,P}} - Q_{L,I} - Q_{L,S} \quad (4)$$

$$Q_{avg,P} = Q_{H,P} + Q_{L,P} \quad (5)$$

The total energy required to produce a part can then be calculated by adding up the power demands of the individual phases multiplied by the time the machine spends in each phase. The warm up energy is amortized over the number of parts that are printed without significant downtime. The machine transitions from standby to warm up, if the downtime exceeds the amount of idle time the controller (likely the thermal limits) is set to allow. This causes the warm up routine to run again, thus it is only included when transitioning from standby to warm up.

$$E_{part} = \sum_{j=P,I,S} \left(Q_{avg,j} * t_{o,j} \right) + \frac{Q_{avg,W} * t_{o,W}}{N_{parts}} \quad (6)$$

In the detailed examination of the Objet Connex350, total energy of producing a part depends heavily on the printing time. Printing time is a function of part volume and the number of sections, fig. 5, the part spans. Power consumption during printing is roughly constant, but the time to print follows a decaying exponential relationship with increased area shown in eq. (8)

$$E_{part}^{Objet} = \overline{P}t = \overline{P}\left(\frac{k}{A} + b \right) Vn \quad (7)$$

$$t \propto \left(\frac{k}{A} + b \right) \quad (8)$$

$$E_{part}^{Objet} \propto \left(\frac{k}{A} + b \right) \quad (9)$$

Where k and b are machine specific constants; A is the nominal area of the X-Y plane used for printing; V is the print volume of the part, and n is the number of sections spanned. The energy consumption of this machine follows a similar trend to that of milling machines in [13], such that the tare energy of the machine is amortized over longer operation. Print time scales with print area, part height and number of sections spanned at different rates resulting in a compounding effect as the part size increases. Additionally, as the part size decreases, the amount of time spent zeroing the print heads and checking the print area becomes a significant fraction.

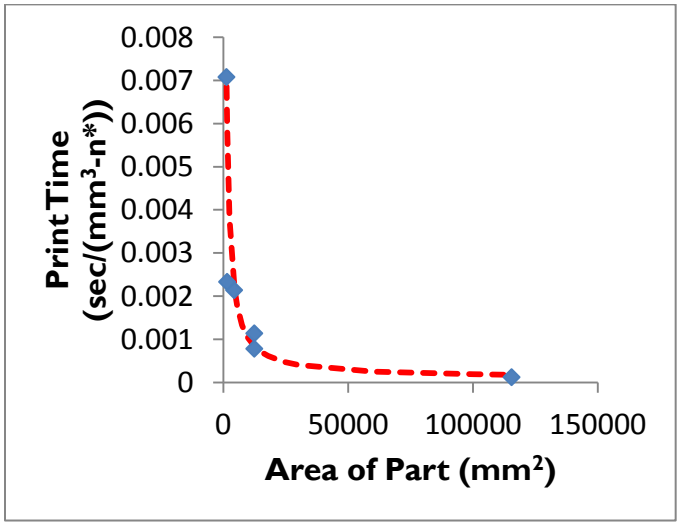

Fig. 5: Energy consumption is directly proportional to print time, which is found to be related to part area according to eq. (7) with k=9.5, b = 0.0001. *For the y-axis, n is the number of print sections spanned

Tab. 1: Summary power consumption by phase for all machines with percentage error in parentheses. Sparse and solid refer to printing settings for part layup.

Power Contribution by Phase		*Standby Power (W)*	*Idle Power (W)*	*Warm-up Power (W)*	*Printing Process Power (W)*	*Total Printing Power (W)*	*Printing Time (s)*	*Test Part Energy (Wh)*	*Initial Purchase Cost ($)*
Objet Connex350		160(1%)	50(42%)	350	530	740(5%)	1700	350	300,000
MakerBot Replicator 2		10 (15%)	20(6%)	170	170	200(20%)	1060	60	2,200
Dimension 1200SST		160(14%)	240(11%)	690	140	540(12%)	870	130	35,000
Dimension 1200BST	*Sparse*	150(17%)	310(6%)	610	100	560(6%)	810	130	30,000
	Solid	150(17%)	310(6%)	860	220	690(5%)	890	170	
uPrint	*Sparse*	130(6%)	300(6%)	400	90	520(8%)	930	130	20,000
	Solid	130(6%)	300(6%)	770	80	510(7%)	910	130	

The parameter k represents the rate at which the machine reduces the effects of tare power on total energy consumption. The parameter b represents a minimum tare contribution to energy consumption.

Quality Results and Description

Dimensional accuracy, resolution and surface roughness, are highly interdependent in AM technologies and serve as the bases of precision. Prior research on AM concludes decreasing layer thickness gives results with better dimensional accuracy [14]. Moreover, dimensional accuracy levels vary across rapid manufacturing technologies and are directly influenced by process parameters other than layer thickness [15] [16]

The reported resolution of the machines varies by completeness. The Objet Connex 350 advertises resolution of 1600 dpi (16 um) in the z-axis and 600 dpi (42 um) in the x and y axes. MakerBot reports 100 um (0.00394 in). Dimension SST 1200, BST and uPrint each report a best layer thickness of 0.254mm (0.010 in).

Tab. 2: Percentage of design slot length achieved before wall adhesion in two orthogonal print directions

Design Length Achieved (%)			
Machine		*X-direction*	*Y-direction*
Objet Connex350		64	55
MakerBot Replicator 2		40	40
Dimension SST		63	61
Dimension 1200BST	Solid	61	61
	Sparse	59	57
uPrint	Solid	62	58
	Sparse	62	59

With regards to the control part, results from most machines are of poor quality and most features that were meant to be measured and compared were not printed or resolved. In some cases, the machine attempts to print such features; in others, the software did not even process features below the programmed resolution of the machine. Generally, features below 500 um are not printed or are printed with poor quality. What was intended to be a sloping ramp, introduced to confirm and analyze the stair effect inherent in deposition processes, was in fact printed as in all but one case, that of the Objet Connex350. The Objet Connex350 printed a ramp with surface roughness consistent with that of the flat face of the control part and with relatively sharp corners compared to other machines.

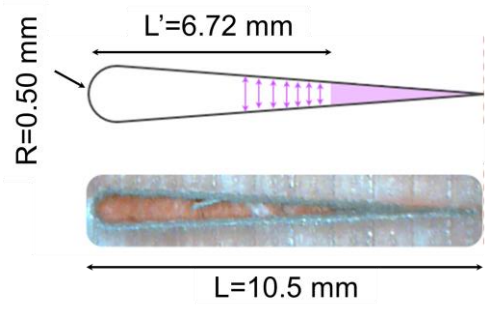

Fig. 6: Diagram showing wall adhesion in printed slot from Objet Connex350 part where L' is achieved length, L is design length

The results for slots printed in the X and Y directions are tabulated in tab. 2 along with a diagram in fig. 6. Two slots started out at a radius of 0.5 mm and two slots started with a radius of 0.25 mm (i.e. a 1 and 0.5 mm initial gap width, respectively). All slots tapered down to zero gap width over a length of 10 mm. Measurement of the printed and fully open slot length provides a basis for comparing resolution of the tested machines. Fig. 6 shows the resolving slot length between the different machines. Even though the Objet Connex350 qualitatively and quantitatively outperformed the other machines, it achieved only slightly better resolution

than the other machines when identifying the smallest possible gap thickness before the gap walls adhere to each other. Determining the designed width of the slot at the location where the printed slot self-adhered indicates the smallest gap width the machine is able to print. Those results are shown in fig. 7 and the resolutions ranged from 400 to 600 µm.

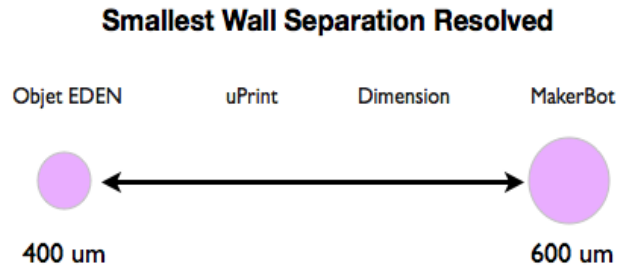

Fig. 7: Range of smallest possible printing resolution achieved by the four machines types that were tested

The spherical dome and groove also demonstrate dimensional accuracy. The spherical groove was printed with poor quality and on multiple machines did not resemble the designed feature, but rather an amorphous divot. Measuring the curvature of the sphere was not achieved. However, it was possible to measure and compare the half-sphere diameter. Tab. 3 shows a comparison of the printed diameter and the design diameter for all machines. The Objet Connex350 stood out with accurate dimensions and excellent resolution when relative to all other machines. The Objet Connex350 accurately printed the design diameter, and also achieved recognizable curvature with a smooth surface finish. The other machines printed a cylinder or blob. The curvature of these other shapes was not obtained.

Tab. 3: Percentage of design diameter achieved for a positive dome and negative divot feature of 1.5 mm each

Design Diameter Achieved (%)			
Machine		*Dome*	*Divot*
Objet Connex350		109	100
MakerBot Replicator 2		58	63
Dimension 1200SST		86	74
Dimension 1200BST	Solid	63	57
	Sparse	89	135
uPrint	Solid	89	144
	Sparse	83	90

Overall, the quality analysis on printed control parts yielded insight into the relative resolution and dimensional accuracy of commercially available AM machines. The machines tested are not able to print at the micron scale with the precision of common micromachining processes.

Combined Results

Combining the results from both the quality assessment of surface roughness and the calculation of total printing energy gives the data points in fig. 8. This generally shows that for a higher quality (lower surface roughness) part, more energy is required. Other factors, not considered in this analysis, may also play a role for the resulting relationship in fig. 8. For example, the Dimension SST1200 is five years newer than the Dimension BST1200 and the uPrint, hence it shows a better energy efficiency for a similar part quality due to advances in energy management and motor control.

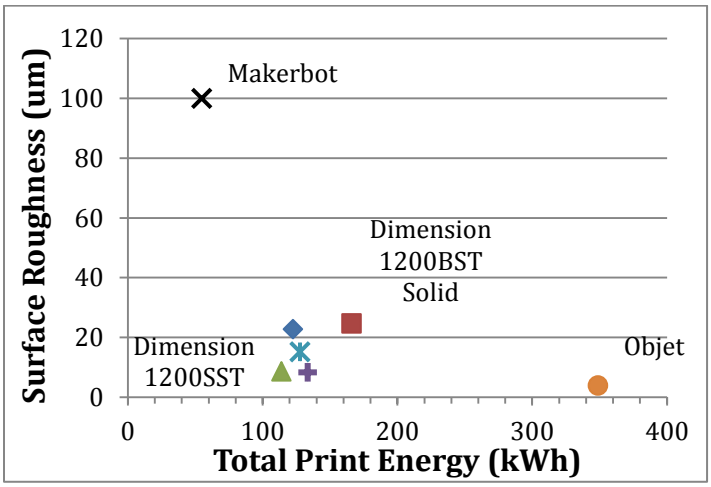

Fig. 8: Total printing energy for control part plotted against worse of orthogonal surface roughness measurements. MakerBot Replicator 2 could not be resolved on the measurement equipment, indicating Ra values greater than 100 um.

CONCLUSIONS

In this study, a methodology is developed to analyze energy consumption in AM. It was concluded that power consumption in AM follows a distinct pattern comprised of standby, warm up, printing and idle phases. Moreover, the bulk of energy consumption was attributed to keeping the heater on in the machine rather than the actual printing process. The results of this study suggest that higher part quality, in terms of surface roughness, requires additional energy investment. Part quality and feature resolution, although varying across the machines, have minimum achievable resolution which may be a function of parameters not explicitly measured in this study. Additionally, the reported resolution of the machines does not well represent the product surface quality. Energy demanded for additive manufacturing depends on the individual characteristics of the machine and the time taken to print the part. For a given machine the part size, and therefore build time, is the primary factor in determining energy requirements. Feature

realization at successively finer length scales requires successively larger capital and resource investment. Marked changes are needed if improved quality is to be realized. The energy and quality assessment methods developed in this paper are applicable to a greater variety of additive manufacturing technologies and will assist designers as additive manufacturing becomes more production friendly. This paper promotes a standard energy data assessment in additive manufacturing processes to consistently educate users about their energy consumption.

FUTURE WORK

Additional testing of the machines in this study for the same part and a variety of parts is needed to assure repeatability of the results and more confidently assert the suggested conclusions. The relationship between additional factors (exact material properties, machine age, etc.) not included in this study and part quality should also be explored for completeness. A larger number of machines could be tested using a similar methodology to make the findings more comprehensive and definitive. On the basis of these results, the energy efficiency of additive manufacturing processes could be improved. In addition, highly energy intensive processes could be demarcated and corresponding technologies could be upgraded.

ACKNOWLEDGMENTS

Athulan Vijayarghavan – System Insights
Karl Walczak – Lawrence Berkeley National Laboratory, Joint Center for Artificial Photosynthesis
David Rolfe* - Marvell Nanofabrication Laboratory
Seungchoun Choi* - Marvell Nanofabrication Laboratory
Scott McCormick* – ME Student Machine Shop
Moneer Helu* – Laboratory for Manufacturing and Sustainability
*University of California, Berkeley

REFERENCES

[1] M. Baumers, C. Tuck, D. L. Bourell, R. Sreenivasan and R. Hague, "Sustainability of additive manufacturing: measuring the energy consumption of the laser sintering process.," *Proceedings of the Institution of Mechanical Engineers, Part B: Journal of Engineering,* pp. 225:2228-2239, 2011.

[2] "ASTM Committee F42 on Additive Manufacturing Technologies," The Free Library, 2010. [Online]. Available: http://www.thefreelibrary.com/ASTM Committee F42 on Additive Manufacturing Technologies.-a0218599226. [Accessed 03 December 2012].

[3] Y. Luo, Z. Ji, M. C. Leu and R. Caudill, "Environmental Performance Analysis of Solid Freeform," in *Proceedings of the 1999 IEEE International Symposium on Electronics and the Environment*, New York, 1999.

[4] M. Baumers, C. Tuck, R. Wildman, I. Ashcroft and R. Hague, "Energy inputs to additive manufacturing: does capacity utilization matter?," *EOS,* 2011.

[5] A. Dietmair and A. Verl, "A generic energy consumption model for decision making and energy efficiency optimisation in manufacturing," *International Journal of Sustainable Engineering,* pp. 123-133, 2009.

[6] V. Balogun and P. Mativenga, "Modelling of direct energy requirements in mechanical machining processes," *Journal of Cleaner Production,* vol. 41, pp. 179-186, 2012.

[7] T. Gutowski, J. Dahmus and A. Thiriez, "Electrical Energy Requirements for Manufacturing Processes," in *13th CIRP International Conference on Life Cycle Engineering*, Leuven, 2006.

[8] W. Li and S. Kara, "An empirical model for predicting energy consumption of manufacturing processes: a case of turning process," *Journal of Engineering Manufacture,* 2011.

[9] A. Vijayaraghavan and D. Dornfeld, "Automated Energy Monitoring of Machine Tools," *CIRP Annals - Manufacturing Technology,* vol. 59, pp. 21-24, 2010.

[10] A. Vijayaraghavan and R. Resnick, "NCDMM Baseline Energy Consumption," LiveBetter Magazine, 2012.

[11] A. Elliott, O. Ivanova, C. Williams and T. Campbell, "An Investigation of the Effects of Quantum Dot Nanoparticles on Photopolymer Resin for Use in Polyjet Direct 3D Printing," *Proceedings of the 2012 SFF SSymposium,* 2012.

[12] H. C. Mohring and P. Kersting, *Research Affiliates Round Robin Testpart Proposal "pc",* Paris: CIRP Research Affiliates Meeting, 2011.

[13] N. Diaz, E. Redelscheimer and D. Dornfeld, "Energy Consumption Characterization and Reduction Strategies for Milling Machine Tool Use," *Globalized Solutions for Sustainability in Manufacturing,* pp. 263-267, 2011.

[14] F. Petzoldt, H. Pohl, A. Simchi and B. Alcantara, "DMLS gets an expert once-over," *Metal Powder Report,* vol. 61, no. 4, pp. 10-13, 2006.

[15] P. M. Hackney, "An investigation into the characteristics of materials and processes, for the production of accurate direct parts and tools using 3D rapid prototyping technologies," Northumbria University, 2007.

[16] M. W. Khaing, J. Y. H. Fuh and L. Lu, "Direct metal laser sintering for rapid tooling: processing and characterisation of EOS parts," *Journal of Materials Processing Technology,* vol. 113, no. 1, pp. 269-272, 2001.

